Archives of Microbiology (2021) 203:5491–5507
https://doi.org/10.1007/s00203-021-02518-w

ORIGINAL PAPER

Plant compounds and nonsteroidal anti-inflammatory drugs interfere with quorum sensing in *Chromobacterium violaceum*

Erika Lorena Giraldo Vargas[1] · Felipe Alves de Almeida[2] · Leonardo Luiz de Freitas[1] · Uelinton Manoel Pinto[3] · Maria Cristina Dantas Vanetti[1]

Received: 15 September 2020 / Revised: 21 July 2021 / Accepted: 6 August 2021 / Published online: 21 August 2021

Abstract

Chromobacterium violaceum is a Gram-negative, saprophytic bacterium that can infect humans and its virulence may be regulated by quorum sensing via *N*-acyl homoserine lactones. A virtual screening study with plant compounds and nonsteroidal anti-inflammatory drugs for inhibition of *C. violaceum* quorum sensing system has been performed. In vitro evaluation was done to validate the in silico results. Molecular docking showed that phytol, margaric acid, palmitic acid, dipyrone, ketoprofen, and phenylbutazone bound to structures of CviR proteins of different *C. violaceum* strains. Phytol presented higher binding affinities than AHLs and furanones, recognized inducers, and inhibitors of quorum sensing, respectively. When tested in vitro, phytol at a non-inhibitory concentration was the most efficient tested compound to reduce phenotypes regulated by quorum sensing. The results indicate that in silico compound prospection to inhibit quorum sensing may be a good tool for finding alternative lead molecules.

Keywords Ketoprofen · Margaric acid · Palmitic acid · Quorum quenching · Violacein

Introduction

Quorum sensing is a process of bacterial cell–cell communication in which cells produce, detect, and respond to extracellular signaling molecules called autoinducers. Gram-negative bacteria typically use *N*-acyl homoserine lactone (AHL), also called autoinducer-1 (AI-1), that can diffuse into the local environment (Reading and Sperandio 2006; Ng and Bassler 2009). Signal concentration increases with population density and, once the AHLs concentration reaches a threshold level, these signals bind to their cognate intracellular receptors, in this case, the LuxR-type family of transcriptional regulators. The activated LuxR-type receptors alter gene expression levels, including a range of phenotypes such as sporulation, biofilm formation, motility, bacteriocin and toxin production, conjugation, competence, virulence gene expression, pigment, and bioluminescence production, among others (Nealson et al. 1970; Fuqua et al. 1994; Geske et al. 2007; Raina et al. 2009; Li and Nair 2012; Boursier et al. 2018).

Chromobacterium violaceum, a Gram-negative water and soil bacterium, can infect humans and cause abscesses and bacteremia (Stauff and Bassler 2011). This bacterium produces the antibacterial purple pigment violacein, synthesized from tryptophan by the products of the *vioABCD* operon, which is regulated by quorum sensing mediated by AIs-1 (Stauff and Bassler 2011). In *C. violaceum,* the AIs-1 are synthesized via the CviI/CviR system, a LuxI/LuxR homolog, where CviI is an AHL synthase, and CviR is a receptor that, when bound to AHLs, modulates the regulation of target genes. CviR is a homodimeric protein, each monomer of which consists of two domains, a ligand-binding domain (LBD) and a DNA-binding domain (DBD), a feature typical of LuxR-type transcription regulators (Choi and Greenberg 1991; Hanzelka and Greenberg 1995; Pinto and Winans 2009).

Communicated by Erko Stackebrandt.

✉ Maria Cristina Dantas Vanetti
mvanetti@ufv.br

[1] Department of Microbiology, Universidade Federal de Viçosa (UFV), 36.570-900, Viçosa, MG, Brazil

[2] Department of Nutrition, Universidade Federal de Juiz de Fora (UFJF), 35.032-620, Governador Valadares, MG, Brazil

[3] Department of Food and Experimental Nutrition, Food Research Center, Universidade de São Paulo (USP), 05.508-900, São Paulo, SP, Brazil

C. violaceum ATCC 12472 is the type strain of the species and produces and responds to AHLs, mainly *N*-(3-hydroxydecanoyl)-DL-homoserine lactone (3-OH-C10-HSL) (Morohoshi et al. 2008). However, several other AHLs have been detected in this strain, with of the acyl chain length ranging from 9 to 12 carbons and containing a 3-oxo or 3-hydroxy function (Mion et al. 2021). *C. violaceum* ATCC 31532, recently reclassified as *Chromobacterium subtsugae* ATCC 31532 by Harrison and Soby (2020), mainly produces *N*-hexanoyl-DL-homoserine lactone (C6-HSL) (McClean et al. 1997; Chen et al. 2011). *C. violaceum* CV026, a biosensor commonly used to evaluate AHL quorum sensing signals, is a mini-Tn5 *civI* mutant derived from wild-type *C. violaceum* ATCC 31532, unable to produce AHL, but retaining the ability to respond to exogenous AHLs (McClean et al. 1997). Wild-type and biosensor mutant strains of *C. violaceum* have been used as models in various studies related to bacterial communication and quorum sensing inhibition, known as quorum quenching (McClean et al. 1997; Adonizio et al. 2006; Vattem et al. 2007; Ravichandran et al. 2018).

The discovery of the quorum sensing system and its critical role in bacterial survival and virulence has revealed a promising approach to attack and attenuate bacterial pathogenicity. The significant advantage of this novel strategy for anti-infective therapy is that it circumvents the problem of antibiotic resistance, which is intimately connected to the use of conventional antibacterial agents, as it specifically interferes with the expression of pathogenic traits rather than to hamper bacterial growth (Singh et al. 2017; Ravichandran et al. 2018; Chbib 2020). Furanones are compounds produced by the red seaweed *Delisea pulchra*, which have been widely studied for acting as antagonists of AHLs and, therefore, inhibit phenotypes regulated by quorum sensing in bacteria (Givskov et al. 1996; Shetye et al. 2013; Choi et al. 2014). Furanones and other AHL analogs are supposed to bind competitively to the LuxR-type receptor proteins and prevent binding of the AHLs to these cognate transcriptional regulators (Givskov et al. 1996).

Plant compounds and nonsteroidal anti-inflammatory drugs (NSAIDs), substances used in the medical field for other purposes, have been screened for their interference with quorum sensing mechanisms (Adonizio et al. 2006; El-Mowafy et al. 2014; Singh et al. 2017). As examples, Chaudhari et al. (2014) investigated the effect of seed extracts of three different plants on quorum sensing and showed inhibition of violacein production in *C. violaceum* and reduced motility in *Pseudomonas aeruginosa*, both mechanisms regulated by AHLs. Ibuprofen and tenoxicam, two NSAIDs, decreased the production of virulence factors regulated by quorum sensing such as pyocyanin, rhamnolipids, proteases, and elastase of *P. aeruginosa* PAO1 (Dai et al. 2019; Askoura et al. 2020).

Considering that some genes and virulence factors in bacteria have been known to be influenced by quorum sensing, the prospection of inhibitors of this mechanism is of interest. Molecular docking has been a commonly used tool in quorum sensing inhibition studies to suggest binding sites between signal receptor proteins and autoinducers, as well as in the search for possible quorum quenching compounds from different sources (Capilato et al. 2016; Almeida et al. 2018; Ding et al. 2018; Ravichandran et al. 2018). For example, Ravichandran et al. (2018) performed a virtual screening of different compounds in *C. violaceum*, and it was reported that quorum sensing inhibitors and the natural AI-1 showed a high binding affinity for the CviR protein. Also, Almeida et al. (2018) performed a virtual screening of 107 plant compounds and 73 NASIDs for inhibition of biofilm formation in *Salmonella enterica* serovar Enteritidis PT4 578. They showed that these compounds bound in at least one of three modeled structures of the SdiA protein, an analog of LuxR, acting as possible inhibitors of the quorum sensing mechanism.

Considering the importance of studies focused on the screening of quorum sensing inhibitory compounds, the present work aimed to perform molecular docking of plant compounds and NASIDs, as well as AHLs and furanones with structures of CviR protein from different strains of *C. violaceum* to prospect quorum sensing inhibitors. Additionally, we have evaluated the in vitro activity by probing violacein production, biofilm formation, cell aggregation, and alkaline protease activity in the presence of these compounds.

Materials and methods

In vitro comparison of the ligand-binding domain (LBD) of structures of CviR proteins

The structures of CviR proteins of *C. violaceum* ATCC 12472 (PDB: 3QP6, 3QP8) and *C. violaceum* ATCC 31532 (PDB: 3QP1, 3QP2, 3QP4, 3QP5) from Chen et al. (2011) were obtained from the RCSB Protein Data Bank database (PDB; http://www.rcsb.org/pdb/home/home.do) (Table 1) and superposed to compare the ligand-binding domain (LBD) by CLC Drug Discovery Workbench 4.0 software.

Amino acid sequences of the CviR proteins of strains of *C. violaceum*

The amino acid sequences of CviR proteins of *C. violaceum* ATCC 12472 (UniProtKB: Q7NQP7) and *C. violaceum* ATCC 31532 (UniProtKB: D3W065) were obtained from the UniProt Knowledgebase database (UniProtKB; https://www.uniprot.org/) and aligned by "ClustalW" tool of the

Table 1 Structures of CviR proteins of *C. violaceum* ATCC 12472 and *C. violaceum* ATCC 31532 obtained from the PDB database and effect observed when bound to different compounds

Bacterial strains	PDB ID	PDB description	Effect of compound
C. violaceum ATCC 12472	3QP6	CviR bound to C6-HSL	Inhibitor
	3QP8	CviR bound to C10-HSL	Inducer
C. violaceum ATCC 31532	3QP1	CviR bound to C6-HSL	Inducer
	3QP2	CviR bound to C8-HSL	Weak inducer
	3QP4	CviR bound to C10-HSL	Inhibitor
	3QP5	CviR bound to chlorolactone	Inhibitor

Chen et al. (2011)

CLC Drug Discovery Workbench 4.0 software (https://www.qiagenbioinformatics.com/).

Molecular docking of CviR proteins of *C. violaceum* with different compounds

The compounds selected for this study were four plant compounds, three NSAIDs, 14 AHLs, seven furanones, and 1-octanoyl-*rac*-glycerol (OCL), totaling 29 compounds (Table 2). The plant compounds were classified according to their leading functional group, and the classification of NSAIDs was obtained from the KEGG Drug database (http://www.genome.jp/kegg/drug/) (Table 2). The structures of these compounds were obtained from the compound Identifier of the PubChem database (PubChem CID; https://pubchem.ncbi.nlm.nih.gov/https://pubchem.ncbi.nlm.nih.gov/) for molecular docking.

The molecular docking of structures of CviR proteins of *C. violaceum* ATCC 12472 and *C. violaceum* ATCC 31532 (Table 1) was performed with compounds (Table 2) using the "Dock Ligands" tool of the CLC Drug Discovery Workbench 4.0 software, with 1000 interactions for each compound and its conformation was changed during the docking via rotation around flexible bonds. The score generated is related to the potential energy change when the protein and the compound come together based on hydrogen bonds, metal ions, and steric interactions, where more negative scores correspond to higher binding affinities (Almeida et al. 2016, 2018).

Subsequently, the results of molecular docking were also used to assess the accommodation of the compounds that showed the best inhibition of violacein production, according to item "In vitro quorum quenching activity in *C. violaceum*", in the pocket of structures bound to natural AI-1 of each strain, 3QP8 (CviR bound to C10-HSL) for *C. violaceum* ATCC 12472 and 3QP2 (CviR bound to C6-HSL) for *C. violaceum* ATCC 31532.

Bacterial strains and standardization of the inoculum

The bacterial strains used for quorum sensing in vitro assays were *C. violaceum* ATCC 12472 and *C. violaceum* CV026. The cultures were stored at − 20 °C in Luria Bertani broth (LB broth; Sigma-Aldrich, USA) supplemented with 40% (v/v) of sterilized glycerol. Before each experiment, *C. violaceum* strains were cultured in LB broth for 48 h at 30 °C, following another cultivation step in the same conditions for 18 h. These cultured were centrifuged at 10,000 g at 4 °C for 10 min, washed with phosphate-buffered saline (PBS; 10 mM, pH 7.2), and standardized to an optical density at 600 nm (OD 600 nm) of 0.1 using a spectrophotometer (Thermo Fisher Scientific, Finland) obtaining the standardized inoculum. In all experiments, the LB broth for *C. violaceum* CV026 growth was supplemented with 20 µg/mL of kanamycin.

Preparation of compounds solution

The subinhibitory concentrations of the plant compounds, NSAIDs, and AHL used in the experiments were based on a preliminary study. These compounds were suspended as described in Table 3 and stored at − 20 °C.

Growth determination

An aliquot of 2 µL of standardized inoculum obtained according to item "Bacterial strains and standardization of the inoculum" was added to 96-well flat-bottomed microplates (TPP, Switzerland) containing 200 µL of LB broth supplemented with plant compounds and NASIDs at the final concentrations shown in Table 3. During incubation at 30 °C, the OD 600 nm was determined in micro-plate reader (Thermo Fisher Scientific, Finland). Cultures grown in the absence of plant compounds and NASIDs were used as controls.

Table 2 Quorum sensing and quorum quenching compounds used for molecular docking with structures of CviR proteins of *C. violaceum* ATCC 12472 and *C. violaceum* ATCC 31532

Group	Classification	Compound	Pubchem CID
Plant compound	Fatty acid	Margaric acid	10465
		Palmitic acid	985
	Oxygenated diterpene	Z-phytol	6430833
		E-phytol	5280435
NSAID	Propionic acid derivative	Ketoprofen	3825
	Pyrazolone derivative	Dipyrone (metamizole)	3111
		Phenylbutazone	4781
AHL	Unmodified in 3-oxo and 3-OH	*N*-dodecanoyl-DL-homoserine lactone	11565426
		N-decanoyl-DL-homoserine lactone	11644562
		N-octanoyl-DL-homoserine lactone	3474204
		N-hexanoyl-DL-homoserine lactone	3462373
		N-butyryl-DL-homoserine lactone	443433
	Modified in 3-oxo	*N*-(3-oxododecanoyl)-L-homoserine lactone	3246941
		N-(3-oxodecanoyl)-L-homoserine lactone	10221060
		N-(3-oxooctanoyl)-L-homoserine lactone	127293
		N-(3-oxohexanoyl)-L-homoserine lactone	688505
	Modified in 3-OH	*N*-(3-hydroxydodecanoyl)-DL-homoserine lactone	11507677
		N-(3-hydroxydecanoyl)-DL-homoserine lactone	71353010
		N-(3-hydroxyoctanoyl)-DL-homoserine lactone	11586792
		N-(3-hydroxyhexanoyl)-DL-homoserine lactone	70185030
		N-(3-hydroxybutyryl)-L-homoserine lactone	10330086
Furanone	Brominated	4-bromo-5-(bromomethylene)-3-dodecyl-2(5H)-furanone	10180544
		4-bromo-5-(bromomethylene)-3-hexyl-2(5H)-furanone	16127328
		4-bromo-5-(bromomethylene)-3-butyl-2(5H)-furanone	9839657
		5-(bromomethylene)-2(5H)-furanone	9877509
		4-bromo-5-(bromomethylene)-2(5H)-furanone	10131246
	Non-brominated	3-butyl-2(5H)-furanone	11768654
		2,2-dimethyl-3(2H)-furanone	147604
OCL	OCL	1-octanoyl-*rac*-glycerol	3033877

NSAID nonsteroidal anti-inflammatory drug, *AHL N*-acyl homoserine lactone, *OCL* 1-octanoyl-*rac*-glycerol

Table 3 Diluents used to prepare the plant compounds, NSAIDs, and AHL and final concentrations used for experiments in the LB broth

Classification	Compound	Company, country	Solvent	Final concentration in LB broth
Plant compound	Phytol	Sigma-Aldrich, USA	Methanol	600 µg/mL
	Margaric acid	Sigma-Aldrich, USA	Isopropanol	600 µg/mL
	Palmitic acid	Sigma-Aldrich, USA	Dimethylsulfoxide	600 µg/mL
NASID	Dipyrone sodium	All Chemistry, Brazil	Sterile water	500 µg/mL
	Ketoprofen	All Chemistry, Brazil	Methanol	500 µg/mL
	Phenylbutazone	Sigma-Aldrich, USA	Acetone	500 µg/mL
AHL	C6-HSL	Sigma-Aldrich, USA	Acetonitrile	10 µM

NSAID nonsteroidal anti-inflammatory drug, *AHL N*-acyl homoserine lactone

In vitro quorum quenching activity in *C. violaceum*

Violacein production, biofilm formation, cell aggregation, and alkaline protease activity of *C. violaceum* were evaluated in LB broth added with plant compounds and NASIDs at the final concentrations described in Table 3. It is noteworthy that, for *C. violaceum* CV026 cultivation, C6-HSL was added at a final concentration of 10 µM (Table 3).

Violacein production was determined by adding 20 µL of standardized inoculum in a microtube containing 1 mL of LB broth supplemented with plant compounds and NASIDs. After 24 h of incubation at 30 °C, growth was evaluated by OD 600 nm in the spectrophotometer, and violacein production quantified according to Blosser and Gray (2000). Briefly, the culture was centrifuged at 10,000 × *g* for 10 min, and the supernatant discarded. The pellet was resuspended in 1 mL of dimethylsulfoxide (DMSO), mixed vigorously for 30 s in a vortex, and centrifuged at 10,000 × *g* for 10 min. An aliquot of 300 µL of supernatant was added to a 96-well micro-plate, and the OD at 585 nm was measured in the spectrophotometer. The violacein production was expressed as the ratio of OD 585/600 nm, which is violacein production per unit of growth (Choo et al. 2006).

Biofilm formation was evaluated using a 96-well flat-bottomed micro-plate. After 30 h incubation, the 96-well plate was emptied, washed with water, stained with 0.1% (w/v) crystal violet, and washed with water, and finally, ethanol was added to dissolve the dye and the OD at 590 nm was determined according to Pimentel-Filho et al. (2014). Biofilm formation was expressed as the ratio of OD 590/600 nm.

The cell aggregation phenotype was determined by adding 150 µL of standardized inoculum in a microtube containing 1.5 mL of LB broth supplemented with plant compounds and NASIDs. After 24 h of incubation at 30 °C, calcium chloride ($CaCl_2 \cdot H_2O$; Dinâmica, Brazil) was added at a final concentration of 1000 µM, and OD at 600 nm was monitored at the start of the experiment (OD1) and after 90 min (OD2) incubation. According to the equation, the percentage of aggregated cells was calculated: % aggregated cells = 100 × (OD1-OD2)/OD1 (Das et al. 2014).

The alkaline protease activity was determined by adding 150 µL of standardized inoculum in a microtube containing 1.5 mL of LB broth supplemented with plant compounds and NASIDs. After 24 h of incubation at 30 °C, the alkaline protease activity of the supernatant was determined according to Howe and Iglewski (1984) and Oca-Mejía et al. (2015) using collagen (Sigma-Aldrich, USA) as substrate. The alkaline protease activity was expressed as the ratio of OD 595/600 nm.

Statistical analyses

Experiments were carried out in three biological repetitions. The values of the triplicates were used for the analysis of variance (ANOVA), followed by Tukey's test using the Statistical Analysis System and Genetics Software (Ferreira 2011). A p value < 0.05 ($p < 0.05$) was considered to be statistically significant.

Results and discussion

Comparison of the ligand-binding domain of CviR proteins

The structures of CviR proteins of *C. violaceum* ATCC 12472 and *C. violaceum* ATCC 31532 crystallized with different AHLs and chlorolactone were superposed and, in general, binding of different ligands to the same protein alters the conformation of the LBD (Fig. 1A, B, C, D). Conformational differences of the LBD were also detected between the CviR proteins of *C. violaceum* ATCC 12472 and *C. violaceum* ATCC 31532 themselves (Fig. 1E, F). Additionally, the amino acid sequence alignment of the CviR proteins of *C. violaceum* ATCC 12472 with *C. violaceum* ATCC 31532 showed 87.55% identity (Fig. S1). Perhaps, this difference in the amino acid sequences of the CviR proteins between these two strains of *C. violaceum* and, consequently, in their three-dimensional conformation, may be related to species identification. Recently, Harrison and Soby (2020) demonstrated by molecular phylogeny tools and metabolic and phenotypic characteristics that *C. violaceum* ATCC 31532 is clearly a member of the species *Chromobacterium subtsugae*. Nguyen et al. (2015) and Almeida et al. (2016) also observed that the structures of SdiA protein of *Escherichia coli* Enterohemorrhagic (EHEC) and the modeled structures of the SdiA protein of *Salmonella* Enteritidis PT4 578 showed slight conformational changes on the LBD and the DBD, depending on the binding to different AHLs. In addition, Nguyen et al. (2015) observed noticeable structural differences at the ligand-binding sites between AHL-bound and -unbound states of EHEC SdiA protein.

Taking into account the changes in protein conformation according to the amino acid sequence and the autoinducer molecule-binding sites with specific amino acids, Chen et al. (2011) showed that in *C. violaceum* ATCC 31532, the non-conserved amino acid M89 is a crucial point for the antagonist or agonist activity of CviR protein when bound to autoinducers. Moreover, a comparison of the C6-HSL, a natural AI-1 of this strain, with *N*-octanoyl-DL-homoserine lactone (C8-HSL), *N*-decanoyl-DL-homoserine lactone (C10-HSL), and chlorolactone complexes revealed that these last molecules cause the side chain of M89 to switch to the "antagonist" position in this protein (Chen et al. 2011). Thus, depending on the quorum sensing signaling molecule that interacts with the

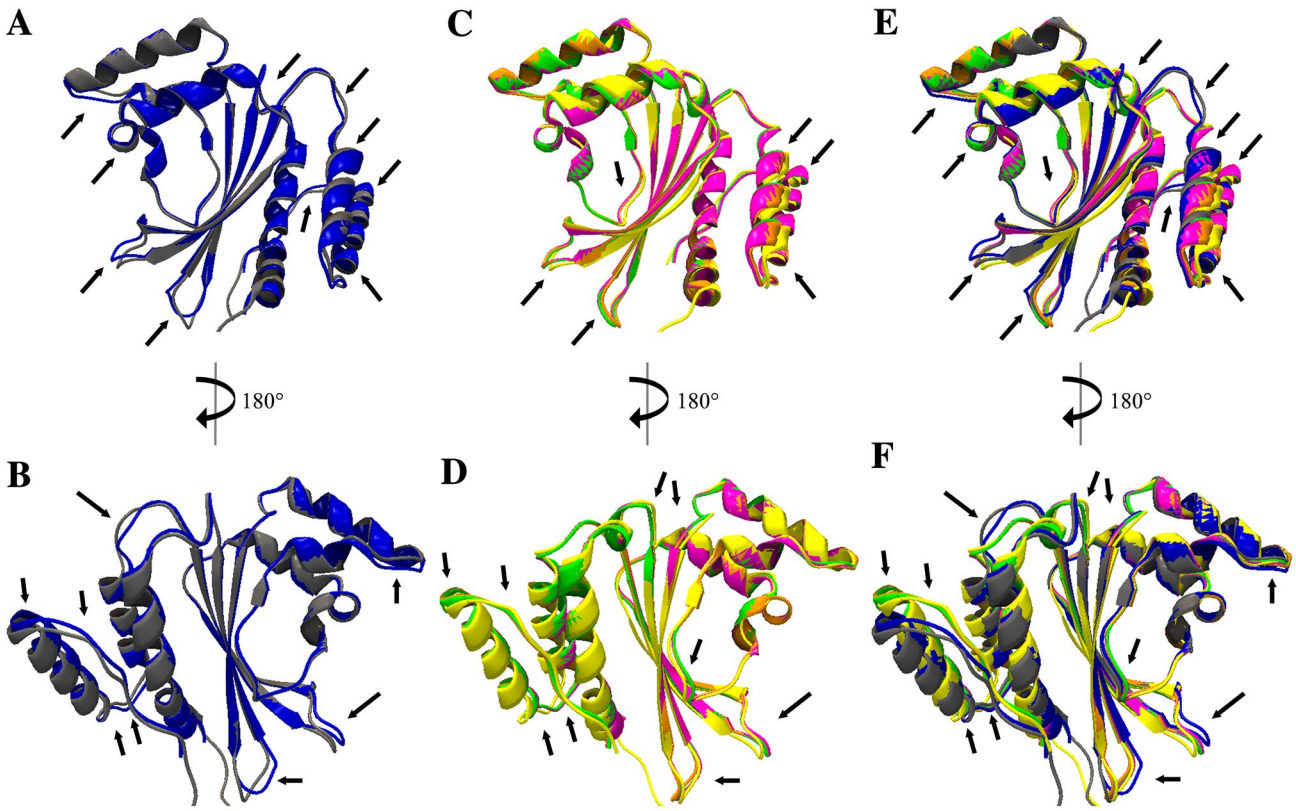

Fig. 1 Superposition of LBD structure monomer of CviR proteins of *C. violaceum.* 3QP6 (CviR bound to C6-HSL; gray) and 3QP8 (CviR bound to C10-HSL; blue) structures of CviR protein of *C. violaceum* ATCC 12472 (**A** and **B**); 3QP1 (CviR bound to C6-HSL; pink), 3QP2 (CviR bound to C8-HSL; orange), 3QP4 (CviR bound to C10-HSL; green), and 3QP5 (CviR bound to chlorolactone; yellow) structures of CviR protein of *C. violaceum* ATCC 31532 (**C** and **D**); conformational differences of the LBD between the CviR proteins of *C. violaceum* ATCC 12472 and *C. violaceum* ATCC 31532 (**E** and **F**). Black arrows show conformational changes (colour figure online)

significant amino acids, the conformation of the CviR protein can change and thus act as an agonist or antagonist of the bacterial communication system (Chen et al. 2011). Therefore, considering that these conformational changes may alter binding affinities with ligands, ultimately altering a quorum sensing response, all structures of the CviR proteins of the two strains were used to perform molecular mechanisms of the two strains docking with different compounds.

Molecular docking of structures of CviR proteins of *C. violaceum* with different compounds

Molecular docking of 3QP6 and 3QP8 structures of the CviR protein of *C. violaceum* ATCC 12472 and of 3QP1, 3QP2, 3QP4, and 3QP5 structures of the CviR protein of *C. violaceum* ATCC 31532 showed that AHLs with 12 carbons, with or without 3-oxo and 3-OH modifications, presented the highest binding affinities (Tables 4 and 5). The AHLs with ten carbons, with the same modifications, also showed high binding affinities with the structures of the evaluated strains (Tables 4 and 5).

It is noteworthy that the 3-OH-C10-HSL showed high binding affinity, reaching a score of -84.80 with 3QP6 structure and -82.24 with the 3QP8 structure of *C. violaceum* ATCC 12472 (Table 4). This AHL is recognized as the most abundant in *C. violaceum* ATCC 12472 (Morohoshi et al. 2008) and induced violacein production in this strain (Morohoshi et al. 2008; Chen et al. 2011). Besides C10-HSL, *N*-dodecanoyl-DL-homoserine lactone (C12-HSL) was also identified as an inducer of violacein production by *C. violaceum* VIR07, an AHL-deficient mutant of *C. violaceum* ATCC 12472 (Morohoshi et al. 2008). Conversely, long-chain acyl AHLs such as C10-HSL and C12-HSL inhibited the production of violacein by *C. violaceum* strain ATCC 31532 (McClean et al. 1997).

AHLs with size chains ranging from four to eight carbons showed lower binding affinities than the AHLs with 10 and 12 carbons with CviR proteins of *C. violaceum* ATCC 12472 and *C. violaceum* ATCC 31532 (Tables 4 and 5). Interestingly, C6-HSL, an AI-1 naturally synthesized by *C. violaceum* ATCC 31532 (McClean et al. 1997; Chen et al. 2011), had one of the lowest binding affinities for the four structures of CviR protein of this strain (Table 5). These results suggest

Table 4 Results of molecular docking of two structures of CviR protein of *C. violaceum* ATCC 12472 with different compounds

Molecule	3QP6			3QP8		
	Binding residue	Score	Rank	Binding residue	Score	Rank
N-(3-hydroxydodecanoyl)-DL-homoserine lactone	Y80, W84, Y88, D97, S155	-89.09	1	Y80, W84, Y88, S155	-88.87	1
N-(3-oxododecanoyl)-L-homoserine lactone	Y80, W84, Y88, D97, S155	-88.55	2	Y80, W84, Y88, D97, S155	-86.09	2
N-dodecanoyl-DL-homoserine lactone	Y80, W84, D97, S155	-88.41	3	Y80, W84, D97, S155	-85.88	3
Z-phytol	M135	-81.57	7	Y88, S89, N92	-83.67	4
N-(3-hydroxydecanoyl)-DL-homoserine lactone	Y80, W84, Y88, D97, S155	-84.80	4	Y80, W84, Y88, S155	-82.24	5
E-phytol	M135	-80.45	8	S89, N92	-81.56	6
N-decanoyl-DL-homoserine lactone	Y80, W84, D97, S155	-81.97	6	Y80, W84, D97, S155	-81.18	7
N-(3-oxodecanoyl)-L-homoserine lactone	Y80, W84, Y88, D97, S155	-83.77	5	Y80, W84, Y88, D97, S155	-80.86	8
4-bromo-5-(bromomethylene)-3-dodecyl-2(5H)-furanone	S155	-77.30	9	Y80, S155	-76.14	9
Margaric acid	L85	-77.19	10	Y88, N92, A94	-74.78	10
N-(3-oxooctanoyl)-L-homoserine lactone	Y80, W84, Y88, D97, S155	-75.68	11	Y80, W84, Y88, D97, S155	-73.99	11
N-octanoyl-DL-homoserine lactone	Y80, W84, S155	-74.88	12	Y80, W84, D97, S155	-73.83	12
Dipyrone (metamizole)	W84	-69.34	16	L85	-72.17	13
Palmitic acid	Y88, A94	-74.21	13	L85	-71.04	14
Ketoprofen	S155	-73.94	14	Y80, S155	-70.54	15
N-(3-hydroxyhexanoyl)-DL-homoserine lactone	Y80, W84, Y88, D97, S155	-69.16	17	Y80, W84, Y88, S155	-69.09	16
N-(3-hydroxyoctanoyl)-DL-homoserine lactone	Y80, Y88, S155	-69.95	15	Y80, Y88, S155	-67.61	17
N-(3-oxohexanoyl)-L-homoserine lactone	Y80, W84, Y88, D97, S155	-67.53	18	Y80, W84, Y88, D97, S155	-66.52	18
N-hexanoyl-DL-homoserine lactone	Y80, W84, D97, S155	-67.10	19	Y80, W84, S155	-66.45	19
1-octanoyl-*rac*-glycerol	Y80, D97, M135, S155	-61.08	20	Y80, D97, M135, S155	-58.40	20
N-(3-hydroxybutyryl)-L-homoserine lactone	Y80, W84, D97, S155	-56.96	21	Y80, W84, S155	-57.06	21
N-butyryl-DL-homoserine lactone	Y80, S155	-51.77	22	Y80, S155	-50.51	22
3-butyl-2(5H)-furanone	W84	-50.57	23	W84	-50.26	23
4-bromo-5-(bromomethylene)-3-butyl-2(5H)-furanone	-	-	-	S155	-49.12	24
5-(bromomethylene)-2(5H)-furanone	Y80	-35.29	24	Y80	-34.36	25
4-bromo-5-(bromomethylene)-2(5H)-furanone	Y80, T140, S155	-34.42	25	W84	-33.58	26
2,2-dimethyl-3(2H)-furanone	Y80	-31.76	26	Y80	-31.12	27
Phenylbutazone	-	-	-	-	-	-
4-bromo-5-(bromomethylene)-3-hexyl-2(5H)-furanone	-	-	-	-	-	-

Rank Binding affinity scale between CviR protein and the compounds with a color ramp ranging from dark pink (higher affinity) to dark green (lower affinity) and hyphen for no binding.

that C10-HSL and C12-HSL can compete more effectively for binding to CviR protein than the C6-HSL and act as inhibitors of violacein production in *C. violaceum* ATCC 31532, as demonstrated experimentally by McClean et al. (1997). Furthermore, our molecular docking results showed that the longer the AHL carbon chain, without 3-oxo and 3-OH modification, the higher the binding affinity with the CviR proteins of *C. violaceum* ATCC 12472 and *C. violaceum* ATCC 31532 (Tables 4 and 5). This result may corroborate previous experimental data of the agonist or antagonistic effect of autoinducer molecules and help to elucidate the molecular mechanism of action.

The 4-bromo-5-(bromomethylene)-3-dodecyl-2(5H)-furanone was the furanone that showed higher binding affinities with the structures of CviR protein of both strains of *C. violaceum*, except to the 3QP5 structure of *C. violaceum* ATCC 31532 (Tables 4 and 5). This brominated furanone also showed binding affinities higher than those of AHLs with a carbon size chain ranging from four to eight, with or without 3-oxo and 3-OH modifications, in *C. violaceum* ATCC 12472, and higher than AHLs of size four to six carbons in *C. violaceum* ATCC 31532 (Tables 4 and 5). This result indicates that this furanone may compete for the CviR -binding site and, consequently, inhibit quorum sensing in *C. violaceum*, as shown in in vitro studies (Ponnusamy et al. 2010; Oliveira et al. 2016). Besides, the two non-brominated furanones evaluated can also bind to CivR protein structures but with low affinities (Tables 4 and 5).

The evaluated plant compounds were able to bind to the structures of the CviR proteins and, the phytol isomers such as Z-phytol and E-phytol showed higher binding affinities (Tables 4 and 5). In *C. violaceum* ATCC 31532, phytol isomers showed higher binding affinities with the four structures of CviR protein, except Z-phytol, which did not bind to the 3QP4 structure (Table 5). These phytol isomers and all evaluated furanones showed higher binding affinities for CviR structures than AHLs with a carbon size chain ranging from six to eight, with or without 3-oxo and 3-OH modification. However, the binding affinities of Z-phytol to the 3QP1 and 3QP2 structures were no higher than AHLs with 12 carbons, with or without 3-oxo and 3-OH modification (Tables 4 and 5). Our in silico studies showed that the binding affinity of Z-phytol was also higher than 3-OH-C10-HSL to the 3QP8 structure, which is the CviR protein

Table 5 Results of molecular docking of four structures of CviR protein of *C. violaceum* ATCC 31532 with different compounds

Molecule	3QP1			3QP2			3QP4			3QP5		
	Binding residue	Score	Rank	Binding residue	Score	Rank	Binding residue	Score	Rank	Binding residue	Score	Rank
N-(3-oxododecanoyl)-L-homoserine lactone	Y80, W84, D97, S155	-84.06	1	Y80, W84, Y88, D97, S155	-84.02	1	Y80, W84, Y88, D97, S155	-84.81	3	Y88, S155	-73.52	4
N-dodecanoyl-DL-homoserine lactone	Y80, W84, D97, S155	-83.12	2	Y80, W84, D97, S155	-82.60	3	Y80, W84, D97, S155	-85.20	1	S155	-74.81	2
N-(3-hydroxydodecanoyl)-DL-homoserine lactone	Y80, W84, D97, S155	-80.77	3	Y80, W84, S155	-83.36	2	Y80, W84, D97, S155	-85.17	2	W84	-71.97	6
N-(3-hydroxydecanoyl)-DL-homoserine lactone	Y80, W84, D97, S155	-79.30	4	Y80, W84, D97, S155	-78.56	8	Y80, W84, D97, S155	-80.54	6	Y88, S155	-68.49	10
Z-phytol	V75	-78.35	5	N92	-79.34	5	-	-	-	N77	-74.16	3
N-decanoyl-DL-homoserine lactone	Y80, W84, D97, S155	-77.75	6	Y80, W84, D97, S155	-78.64	7	Y80, W84, D97, S155	-81.31	5	W84, D97, S155	-70.18	8
N-(3-oxodecanoyl)-L-homoserine lactone	Y80, W84, D97, S155	-77.71	7	Y80, W84, Y88, D97, S155	-79.77	4	Y80, W84, Y88, D97, S155	-81.62	4	W84, Y88, D97, S155	-70.31	7
N-(3-oxooctanoyl)-L-homoserine lactone	Y80, W84, Y88, D97, S155	-74.51	8	Y80, W84, Y88, D97, S155	-72.51	10	Y80, W84, D97, S155	-72.28	11	W84, D97, S155	-63.94	16
E-phytol	V75	-74.40	9	M89	-79.13	6	V75, N77	-76.80	7	L72	-76.70	1
4-bromo-5-(bromomethylene)-3-dodecyl-2(5H)-furanone	W84	-73.80	10	S155	-74.70	9	W84	-76.67	8	-	-	-
N-octanoyl-DL-homoserine lactone	Y80, W84, D97, S155	-73.32	11	Y80, W84, D97, S155	-72.19	11	Y80, W84, D97, S155	-72.78	10	W84, D97, S155	-64.34	15
Dipyrone (metamizole)	W84, Y88	-68.91	12	L85	-70.25	13	L85	-71.22	13	W84	-72.99	5
Margaric acid	M135	-68.62	13	W84	-70.49	12	M135	-72.88	9	M89, N92	-69.31	9
Ketoprofen	Y80, S155	-67.70	14	Y80, S155	-67.71	15	Y80, S155	-70.04	14	Y88	-68.43	11
N-(3-hydroxyhexanoyl)-DL-homoserine lactone	Y80, W84, Y88, D97, S155	-66.86	15	Y80, W84, Y88, S155	-65.81	17	Y80, W84, Y88, D97, S155	-66.47	16	W84, S155	-58.37	19
N-(3-oxohexanoyl)-L-homoserine lactone	Y80, W84, Y88, D97, S155	-66.50	16	Y80, W84, Y88, D97, S155	-64.73	18	Y80, W84, Y88, D97, S155	-66.20	17	W84, Y88, D97, S155	-58.80	18
N-(3-hydroxyoctanoyl)-DL-homoserine lactone	W84, Y88, D97	-65.70	17	Y80, Y88, S155	-66.06	16	Y80, Y88, S155	-67.21	15	Y80	-64.36	14
Palmitic acid	M135	-65.30	18	M89, N92, A94	-68.38	14	Y88, A94	-71.96	12	N92	-65.16	13
N-hexanoyl-DL-homoserine lactone	Y80, W84, D97, S155	-64.90	19	Y80, W84, D97, S155	-63.88	19	Y80, W84, D97, S155	-64.88	18	W84, S155	-57.57	20
4-bromo-5-(bromomethylene)-3-hexyl-2(5H)-furanone	W84	-59.09	20	-	-	-	S155	-59.07	19	-	-	
1-octanoyl-*rac*-glycerol	Y80, M135, S155	-58.10	21	Y80, D97, M135, S155	-58.75	20	L85, Y88	-58.87	20	D97, M135	-59.23	17
N-(3-hydroxybutyryl)-L-homoserine lactone	Y80, W84, Y88, D97, S155	-56.01	22	Y80, W84, Y88, D97, S155	-54.42	21	Y80, W84, S155	-56.12	21	W84	-50.48	22
4-bromo-5-(bromomethylene)-3-butyl-2(5H)-furanone	W84	-51.46	23	W84	-50.04	22	S155	-51.63	22	S155	-52.30	21
3-butyl-2(5H)-furanone	W84	-49.35	24	W84	-48.46	24	W84	-49.83	24	-	-	-
N-butyryl-DL-homoserine lactone	Y80, S155	-49.01	25	Y80	-48.57	23	Y80	-49.90	23	W84	-48.94	23
2,2-dimethyl-3(2H)-furanone	Y80	-35.04	26	-	-	-	Y80	-30.02	26	-	-	-
5-(bromomethylene)-2(5H)-furanone	Y80	-33.14	27	Y80	-33.24	26	-	-	-	W84	-33.41	25
4-bromo-5-(bromomethylene)-2(5H)-furanone	S155	-33.02	28	W84	-34.60	25	Y80, S155	-34.35	25	W84	-36.41	24
Phenylbutazone	-	-		-	-	-	-	-	-	S155	-67.29	12

Rank Binding affinity scale between CviR protein and the compounds with a color ramp ranging from dark pink (higher affinity) to dark green (lower affinity) and a hyphen for no binding

of *C. violaceum* ATCC 12472 crystallized with this inducer (Chen et al. 2011). This may explain the inhibitory effect of phytol on the mechanism of quorum sensing described by other authors in previous in vitro studies (Pejin et al. 2014; Srinivasan et al. 2016, 2017). We also observed that the margaric and palmitic acids had lower binding affinities than those AHLs with carbon size chain ranging from 8 to 12, with or without 3-oxo and 3-OH modifications, in the CviR proteins of two strains of *C. violaceum*, as well as lower than 4-bromo-5-(bromomethylene)-3-dodecyl-2(5H)-furanone (Tables 4 and 5).

Molecular docking performed by Priyanka et al. (2015) showed that margaric acid (PubChem CID: 10465) had a binding affinity with the structure 3QP5 of *C. violaceum* ATCC 31532 lower than *N*-(3-oxohexanoyl)-L-homoserine lactone (3-oxo-C6-HSL) and higher than palmitic acid (PubChem CID: 985) and phytol (PubChem CID: 6437979). In the molecular docking performed by these authors, the compounds previously described showed a lower binding score with the structure of the CviR protein when compared to our results. It is noteworthy that the phytol structure used by these authors is classified as pseudophytol (PubChem CID: 6437979) and different from the structures used in the present study, which were Z-phytol (PubChem CID: 6430833) and E-phytol (PubChem CID: 5280435). Pérez-López et al. (2018) also showed by molecular docking that caproic, caprylic, lauric, myristic, palmitic, stearic, lignoceric, elaidic, oleic, and erucic acids bound in the 3QP1 structure of the CviR protein of *C. violaceum* ATCC 31532. Of these, lauric, myristic, and stearic acids had a greater binding affinity. Another in silico study revealed that Z-phytol, as well as the plant compounds classified as methoxy phenol and fatty acids, such as margaric and palmitic acid, as promising candidates for in vitro tests of quorum sensing inhibition mediated by AI-1, when evaluated by molecular docking with the modeled SdiA protein structures of *Salmonella* Enteritidis PT4 578 (Almeida et al. 2018).

Among the NSAIDs tested, ketoprofen and dipyrone (metamizole) were able to bind in the structures of CivR proteins with lower binding affinities than the AHLs with carbon size chain ranging from 10 to 12, with or without 3-oxo and 3-OH modifications and, the 4-bromo-5-(bromomethylene)-3-dodecyl-2(5H)-furanone. These compounds also showed lower binding affinities than phytol isomers and margaric acid. On the other hand, phenylbutazone did not bind to any of the structures of the CviR protein of *C. violaceum* ATCC 12472 evaluated (Table 4). However, it can bind to the 3QP5 structure of the CviR protein of *C. violaceum* ATCC 31532 crystallized with chlorolactone, an inhibitor of quorum sensing (Table 5). Molecular docking of the modeled structures of the SdiA protein of *Salmonella* Enteritidis PT4 578 with 73 NSAIDs, including ketoprofen, dipyrone, and phenylbutazone, showed that all NSAIDs were able to bind to at least one of the evaluated structures (Almeida et al. 2018). Also, the NSAIDs classified as a pyrazolone derivative, such as phenylbutazone and dipyrone, showed high

binding affinities with the SdiA protein (Almeida et al. 2018). Dai et al. (2019) showed that ibuprofen, an NSAID, bound in LuxR, LasR, RhlR, and PqsR.

In general, although the plant compounds and NSAIDs had a lower binding score than some long acyl chain AHLs, they showed good affinity to the structures of *C. violaceum* CviR protein, which may indicate to be good candidates for in vitro tests on inhibition of violacein production.

Visualization of molecular docking of the quorum quenching compounds in *C. violaceum*

Molecular docking of the 3QP8 structure of the CviR protein of *C. violaceum* ATCC 12472 showed that palmitic acid, margaric acid, and ketoprofen accommodated in this structure in a manner similar to 3-OH-C10-HSL, a natural AI-1 (Fig. 2A–H). The 3-OH-C10-HSL bound to Y80, W84, Y88, and S155 residues of 3QP8 (Fig. 2I), while the palmitic acid bound only to L85 residue (Fig. 2J). On the other hand, margaric acid bound to Y88, N92, and A94 residues (Fig. 2K) and ketoprofen to Y80 and S155 residues (Fig. 2L). Margaric acid has the Y88 residue as a common binding site with 3-OH-C10-HSL in the 3QP8 structure and ketoprofen to the two residues, Y80 and S155. It can be seen that the evaluated compounds bind at near positions in the amino acid sequence, mainly between 80 and 94, similarly to 3-OH-C10-HSL, a natural AI-1, which may indicate that they can compete for the binding site with this signaling molecule.

The molecular docking with the 3QP1 structure of the *C. violaceum* ATCC 31532 CivR protein showed that palmitic acid, margaric acid, and ketoprofen accommodated in the 3QP1 structure in a manner similar to the autoinducer C6-HSL (Figs. 3A–H). The C6-HSL molecule bound to Y80, W84, D97, and S155 residues of

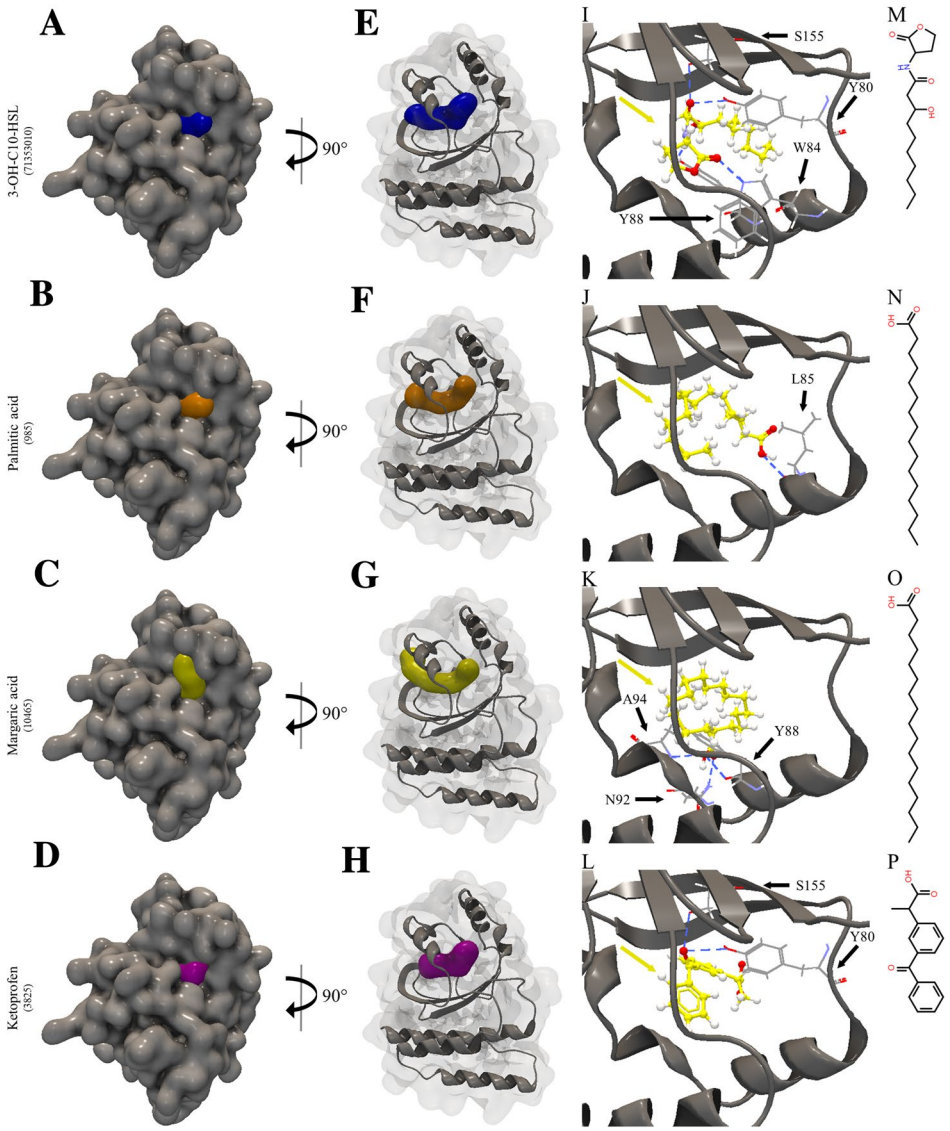

Fig. 2 Molecular docking of 3QP8 structure of CviR protein of *C. violaceum* ATCC 12472 with 3-OH-C10-HSL, palmitic acid, margaric acid, and ketoprofen. Surface representation of 3QP8 structure of CviR protein of *C. violaceum* ATCC 12472 (**A**, **B**, **C**, and **D**), surface and backbone representations (**E**, **F**, **G**, and **H**), backbone representation with a hydrogen bond between the amino acid residues and compounds evaluated (**I**, **J**, **K**, and **L**), and structures of 3-OH-C10-HSL, palmitic acid, margaric acid, and ketoprofen (**M**, **N**, **O**, and **P**). Gray surface representation, CviR protein; Blue surface representation, 3-OH-C10-HSL; Orange surface representation, palmitic acid; Yellow surface representation, margaric acid; Purple surface representation, ketoprofen; Gray backbone representation, CviR protein; Black arrow indicates the binding site; Yellow arrow, 3-OH-C10-HSL or palmitic acid or margaric acid or ketoprofen; Blue dashed line, hydrogen bond (colour figure online)

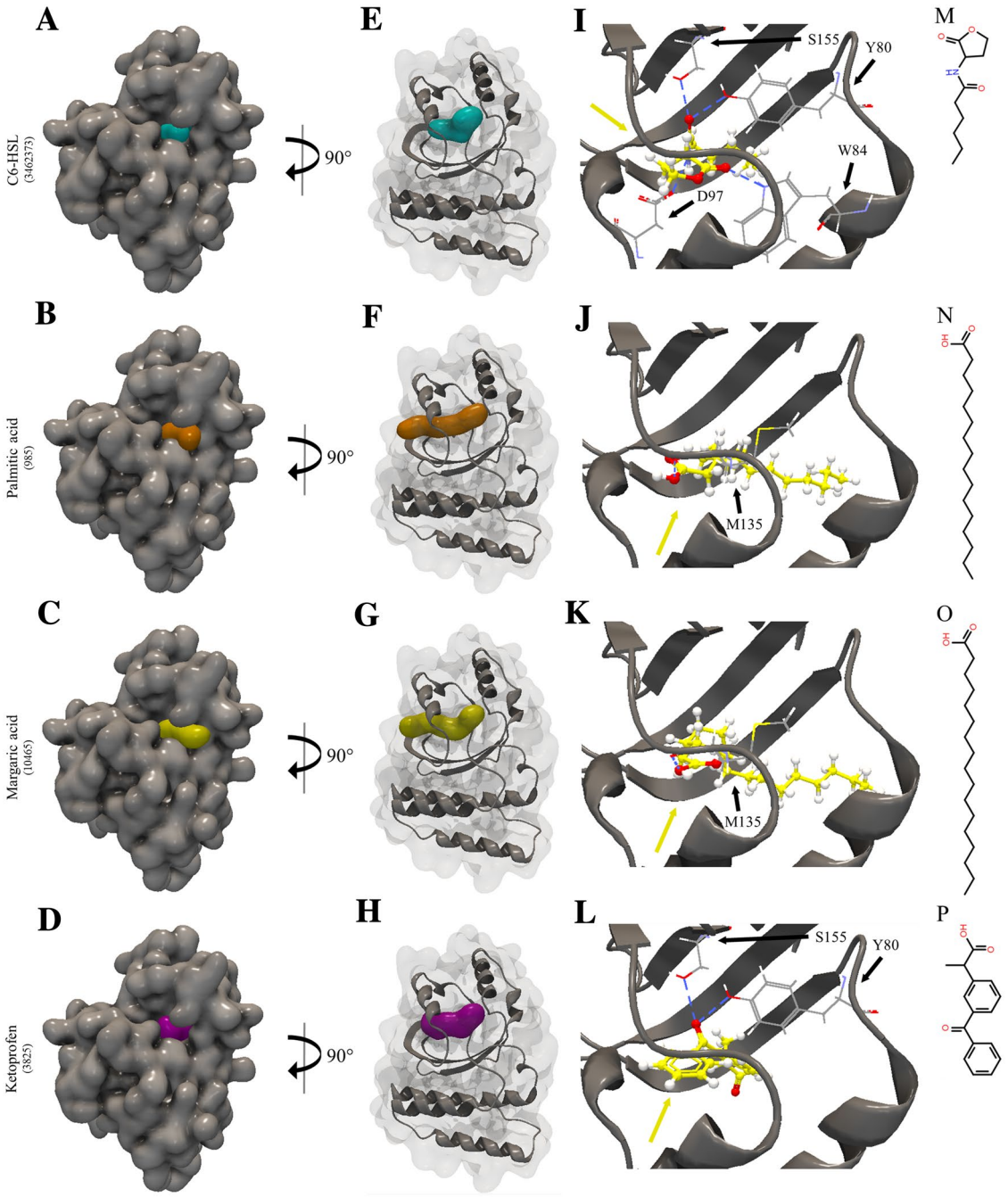

Fig. 3 Molecular docking of 3QP1 structure of CviR protein of *C. violaceum* ATCC 31532 with C6-HSL, palmitic acid, margaric acid, and ketoprofen. Surface representation of 3QP1 structure of CviR protein of *C. violaceum* ATCC 31532 (**A**, **B**, **C**, and **D**), surface and backbone representations (**E**, **F**, **G**, and **H**), backbone representation with a hydrogen bond between the amino acid residues and compounds evaluated (**I**, **J**, **K**, and **L**), and structures of C6-HSL, palmitic acid, margaric acid, and ketoprofen (**M**, **N**, **O**, and **P**). Gray surface representation, CviR protein; Aquamarine surface representation, C6-HSL; Orange surface representation, palmitic acid; Yellow surface representation, margaric acid; Purple surface representation, ketoprofen; Gray backbone representation, CviR protein; Black arrow indicates the binding site; Yellow arrow, C6-HSL or palmitic acid or margaric acid or ketoprofen; Blue dashed line, hydrogen bond (colour figure online)

the CivR protein (Fig. 3I) and these results are in agreement with Ravichandran et al. (2018), which showed the binding of the autoinducer in these same amino acids. Moreover, palmitic and margaric acids bound to M135 residue (Fig. 3J, K), whereas ketoprofen bound to Y80 and S155 residues (Fig. 3L). Thus, this NSAID presented

a binding to amino acid residues that coincide with the binding of the cognate ligand C6-HSL. These results may also indicate that the compounds compete for the binding site with the signaling molecule.

In vitro quorum quenching activity of plant compounds and NSAIDs in *C. violaceum*

The growth measured as OD 600 nm of *C. violaceum* ATCC 12472 and *C. violaceum* CV026 cultured in the presence of plant compounds and NASIDs, at concentrations indicated in Table 1, were compared to the control and were not statistically different ($p > 0.05$) (Fig. S2). The effect of sodium dipyrone sodium was an exception, and although there is a partial growth inhibition, the evaluated phenotypes considered the relationship with the cell population, that is, the data have been normalized per number of cells, and the results are presented below.

Plant compounds

Plant compounds exhibited different effects on the inhibition of quorum sensing-related violacein in two strains of *C. violaceum* (Fig. 4A, E). The palmitic and margaric acids decreased violacein production by *C. violaceum* ATCC 12472 in 60.3% and 41.4% in comparison to the control, respectively ($p < 0.05$), while the phytol compound showed no effect on the production of violacein in this strain (Fig. 4A). However, the presence of phytol, margaric acid, and palmitic acid decreased violacein production by *C. violaceum* CV026 ($p < 0.05$) (Fig. 4E) at 33.6%, 15.2%, and 15.4%, respectively. The highest percentage of inhibition observed in pigment production in *C. violaceum* ATCC 12472 by palmitic and margaric acids may be due to competition with 3-OH-C10-HSL to binding at CviR, since in silico data suggest that these plant compounds bound to the CviR amino acids residues that are very close to the binding sites of the cognate AI-1 produced by this strain (Fig. 2I, J, K). The inability of phytol to inhibit violacein production in *C. violaceum* ATCC 12472 may be associated with the binding affinity to CviR protein, which was lower than C12-HSL and 3-OH-C10-HSL, two cognate AI-1 (Table 4). In contrast, the inhibition of violacein production by *C. violaceum* CV026 by phytol may be related to the higher binding affinity than the cognate AI-1 C6-HSL to the CviR protein (Table 5).

A significant reduction in biofilm formed in the presence of phytol and margaric acid, at a concentration of 600 µg/mL, in both *C. violaceum* strains was observed (Fig. 4B, F). These two natural compounds had higher binding scores than palmitic acid to the CivR protein of both strains of *C. violaceum* (Tables 4 and 5). The reduction in biofilm formation occurred without reducing bacterial growth, and therefore, it could be related to mechanisms other than growth inhibition. Previously, compounds that prevent biofilm formation by *C. violaceum* were suggested to be related to quorum sensing disruption (Burt et al. 2014; Oca-Mèjia et al. 2015). Carvacrol, one of the major antimicrobial components of oregano oil, significantly reduced the biofilm formation by *C. violaceum* at 0.1 mM, without significant reduction in bacterial counts (Burt et al. 2014). The authors indicate that carvacrol's inhibition of biofilm formation may be related to the disruption of quorum sensing.

Phytol and palmitic acid significantly reduced cell aggregation in *C. violaceum* ATCC 12472 and *C. violaceum* CV026 (Figs. 4C, G). A substantial difference in cell aggregation was observed by Oca-Mejìa et al. (2015) for both strains of *C. violaceum*, and the wild-type aggregation was 31% higher that the aggregation observed for *C. violaceum* CV026. However, these authors determined the cell aggregation after 15 h and our results refer to 90 min. Cell aggregation is promoted by quorum sensing in several bacteria (Waters and Bassler 2005) and, in liquid culture, aggregation has been correlated with a propensity to form biofilm communities. Liquid-culture aggregates probably have many of the same characteristics as a biofilm community, including cells held together by an extracellular matrix and steep chemical gradients within the aggregate (Parsek and Greenberg 2005).

Alkaline protease activity seems to be regulated by quorum sensing in *C. violaceum* (Oca-Mejìa et al. 2015). Lower activity of this protease was observed in the supernatant of the *C. violaceum* CV026 compared to *C. violaceum* ATCC 12472, and phytol inhibited alkaline protease activity in both strains (Figs. 4D, H). Interestingly, the presence of margaric and palmitic acids significantly reduced the protease activity in *C. violaceum* CV026 (Figs. 4D, H).

The quorum quenching activity of phytol has been demonstrated in different bacteria (Pejin et al. 2014; Srinivasan et al. 2016, 2017). In subinhibitory concentrations of 0.5, 0.25, and 0.125 of MIC (MIC was 19 µg/mL), phytol reduced the biofilm formation by *P. aeruginosa* in the range of 74–84% (Pejin et al. 2014). This compound also reduced the production of pyocyanin and twitching motility on *P. aeruginosa*, phenotypes recognized as regulated by quorum sensing (Pejin et al. 2014). Srinivasan et al. (2016) showed that phytol interfered with quorum sensing regulated phenotypes in *Serratia marcescens*, as it reduced the prodigiosin production and that the ethyl acetate extract of *Piper betle*, mainly containing phytol at a concentration of 500 µg/mL, decreased prodigiosin production, biofilm formation, swarming motility, production of exopolysaccharide, lipase, and protease. The extract of *P. betle* also reduced biofilm formation, swimming motility, and exopolysaccharide production, as well as inhibited quorum sensing mediated bioluminescence in *Vibrio harveyi* (Srinivasan et al. 2017).

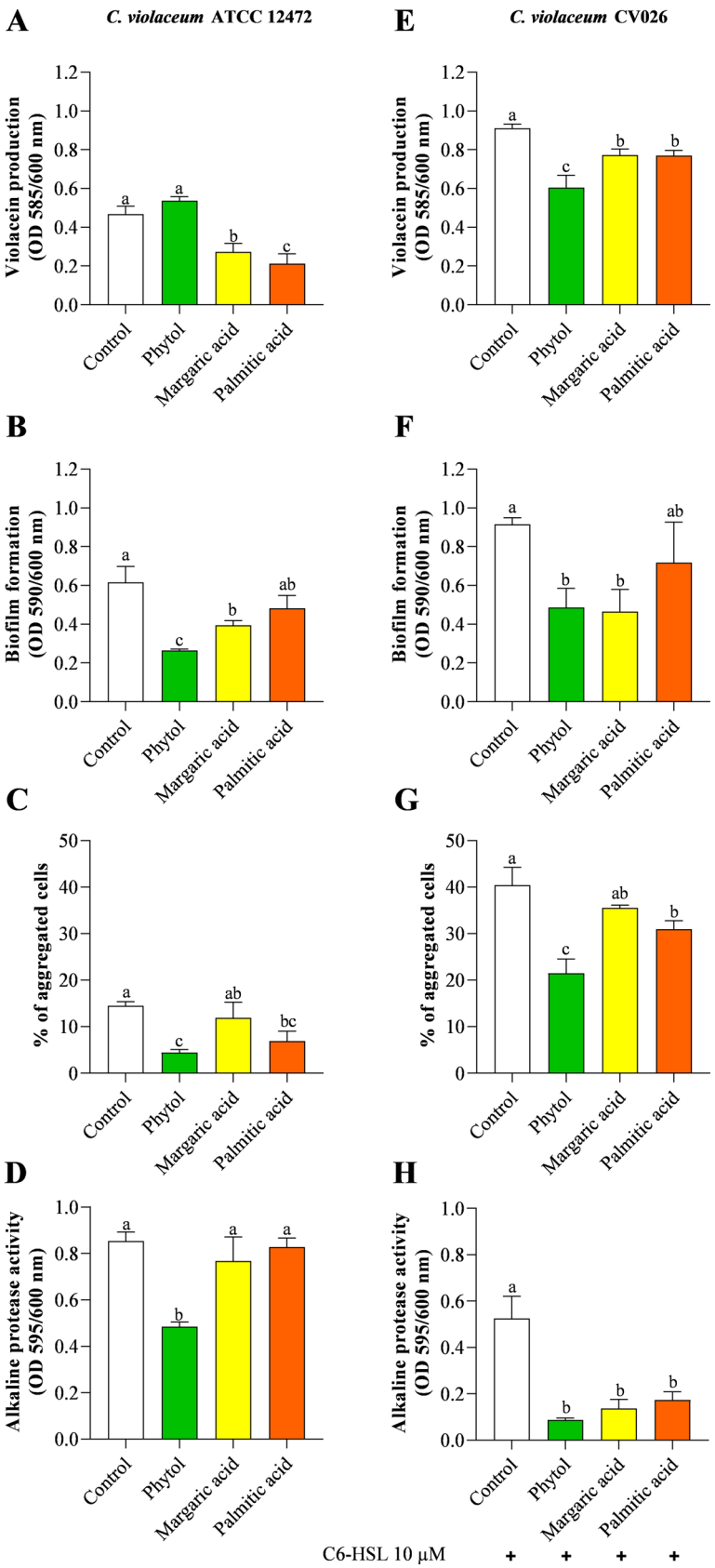

Fig. 4 Violacein production (**A** and **E**), biofilm formation (**B** and **F**), percentage (%) of aggregated cells (**C** and **G**), and alkaline protease activity (**D** and **H**) of *C. violaceum* ATCC 12472 and *C. violaceum* CV026 in the presence of plant compounds, respectively. Control refers to bacterial growth on LB broth. The means followed by different letters differ at 5% probability ($p < 0.05$) by Tukey's test (colour figure online)

Palmitic, linoleic, oleic, and stearic acids can inhibit autoinducer-2 (AI-2) activity and, consecutively, affect quorum sensing (Soni et al. 2008). Myristic, palmitic, and stearic acids did not inhibit swarming motility of *P. aeruginosa* PAO1, but palmitoleic, oleic, vaccenic, and linoleic acids did (Inoue et al. 2008). Sunflower, chia, and amaranth oils containing palmitic, stearic, oleic, and linoleic acids inhibited the production of violacein and alkaline exoprotease activity of *C. violaceum* 553. Lauric, myristic, and stearic acids also inhibited violacein production by 60–84%, and palmitic acid showed non-significant effect (Pérez-López et al. 2018). Marathe et al. (2018) evaluated the inhibitory effect of linoleic acid upon quorum sensing and showed a reduction in urease activity and biofilm formation in *Proteus mirabilis* and also a decrease of protease and prodigiosin synthesis and biofilm formation in *S. marcescens.* The properties as quorum sensing inhibitors and the ease of obtaining these compounds in nature make them attractive sources to be used to combat pathogenic bacteria. Therefore, this is the first evidence that shows margaric and palmitic acid as having an anti-quorum sensing effect and more studies aiming to explore their potential application in foods to control cell-to-cell communication regulated phenotypes in Gram-negative should be performed.

Nonsteroidal anti-inflammatory drugs (NSAIDs)

The NSAIDs showed a low effect on inhibition of violacein production by *C. violaceum* ATCC 12472, and the maximum inhibition observed was 32% with ketoprofen ($p < 0.05$) (Fig. 5A). On the other hand, the three NSAIDs decreased violacein production by *C. violaceum* CV026 ($p < 0.05$), with dipyrone sodium being the most effective with 57.8% reduction, followed by ketoprofen with 38.6% and phenylbutazone with 28.6% reduction (Fig. 5E).

The effect of NSAIDs on biofilm formation by *C. violaceum* ATCC 12472 and *C. violaceum* CV026 varied, with dipyrone sodium and phenylbutazone reducing biofilm formation in the wild-type, and dipyrone sodium and ketoprofen reducing in the mutant strain (Fig. 5B, F). Among the NSAIDs, dipyrone sodium showed the best binding score in the CivR protein of the two strains (Tables 4 and 5) which is also reflected in the biofilm assay as being the most effective.

Different effects of NSAIDs on the two strains of *C. violaceum* were also observed in the cell aggregation phenotype. Phenylbutazone was the only anti-inflammatory agent with a common inhibitory effect on cell aggregation for both strains (Fig. 5C, G). As observed for the plant compounds, there is no correlation between compounds that inhibit aggregation and biofilm formation. However, the complexity of the stages of biofilm formation and the character of the aggregation analyses, which were carried out with 90 min of incubation in the presence of the aggregation factor, must be considered.

Alkaline protease activity from *C. violaceum* ATCC 12472 was slightly reduced by 17.6% in the presence of phenylbutazone, whereas this NSAID also reduced the activity of this protease from *C. violaceum* CV026 by 38.7% (Fig. 5D, H). Additionally, ketoprofen also presented an inhibitory effect on the protease activity of *C. violaceum* CV026 (Fig. 5H).

The quorum quenching effect of NSAIDs was observed in other bacteria, both in in silico and in vitro studies (El-Mowafy et al. 2014; Soheili et al. 2015; Almeida et al. 2018; Dai et al. 2019; Askoura et al. 2020). El-Mowafy et al. (2014) showed that aspirin, a widely used NSAID, reduced the concentration of *N*-butyryl-DL-homoserine lactone (C4-HSL) and *N*-(3-hydroxydodecanoyl)-DL-homoserine lactone (3-OH-C12-HSL) in the supernatant of *P. aeruginosa* culture, as well as reduced production of protease, elastase, hemolysin, and pyocyanin. The NSAIDs ibuprofen and tenoxicam decreased the production of virulence factors regulated by quorum sensing such as pyocyanin, rhamnolipids, proteases, and elastase of *P. aeruginosa* PAO1 (Dai et al. 2019; Askoura et al. 2020).

No studies were found to show the quorum quenching effect of dipyrone sodium, ketoprofen, and phenylbutazone, and this is the first report showing inhibitory ability in a phenotype regulated by quorum sensing in *C. violaceum.*

Not all in silico results could be validated in vitro. Phenylbutazone could not bind to any of the structures of the CviR protein of *C. violaceum* ATCC 12472 but, it inhibits phenotypes as biofilm formation, cell aggregation and alkaline protease activity (Fig. 5A–C). On the other hand, this NSAID bound in silico in one of four structures of the CviR protein of *C. violaceum* ATCC 31532 and downregulated violacein production, cell aggregation, and alkaline protease activity in the mutant strain *C. violaceum* CV026. Thus, although the effects of inhibiting quorum sensing phenotypes by the compounds tested can be in part explained by the results observed in silico, it should be considered that the presence and concentrations of other substances in the media may also interfere with the evaluated phenotypes (Liu et al. 2013; Choi et al. 2015; Mahmoudi 2015). It also needs to be considered that the quorum sensing inhibition could be related with the reduction in the expression of the *cviI* gene that encodes the *N*-acyl-L-homoserine lactone synthase (CviI) or ever to the interference in the activity of the CviI protein.

Conclusion

The evaluated plant compounds and NSAIDs generally had a high binding affinity to the CviR structures of *C. violaceum*. Overall, these in silico prospected compounds showed inhibition of violacein production, biofilm formation, cell aggregation, and alkaline protease activity. These results show

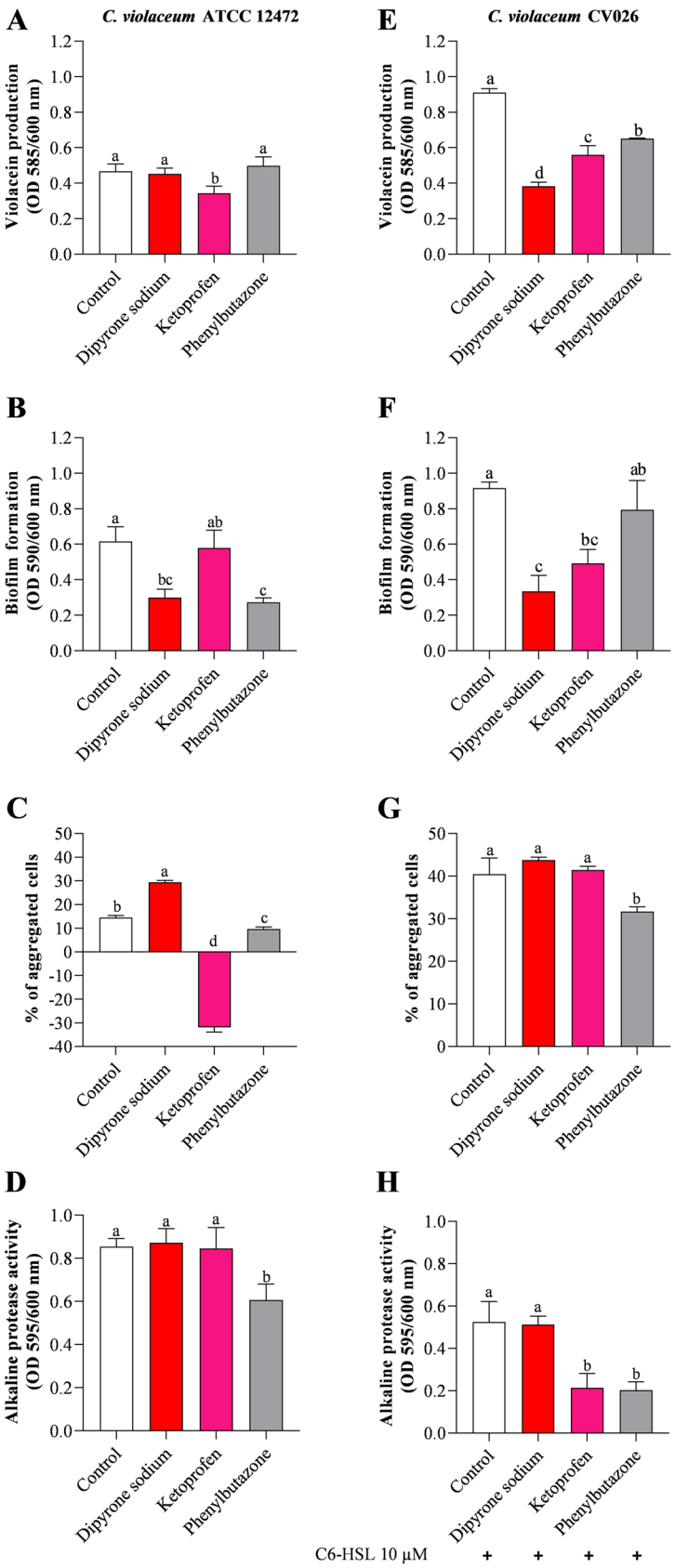

Fig. 5 Violacein production (**A** and **E**), biofilm formation (**B** and **F**), percentage (%) of aggregated cells (**C** and **G**), and alkaline protease activity (**D** and **H**) of *C. violaceum* ATCC 12472 and *C. violaceum* CV026 in the presence of NSAIDs, respectively. Control refers to bacterial growth on LB broth. The means followed by different letters differ at 5% probability ($p < 0.05$) by Tukey's test (colour figure online)

that the combination of in silico tools and in vitro tests is a useful methodology for prospecting quorum quenching compounds, so that molecules with anti-quorum sensing effects can be found in a more effective way to combat pathogens.

Supplementary Information The online version contains supplementary material available at https://doi.org/10.1007/s00203-021-02518-w.

Acknowledgements Erika Lorena Giraldo Vargas was supported by a fellowship from Coordenação de Aperfeiçoamento de Pessoal de Nível Superior (CAPES) and this research has also been supported by CAPES. The authors acknowledge the CLC bio of the QIAGEN Company by the license of the CLC Drug Discovery Workbench 4.0 software.

Funding This research has been supported by Coordenação de Aperfeiçoamento de Pessoal de Nível Superior (CAPES).

Data availability Supplementary information was disponible.

Declarations

Conflict of interest The authors declare no conflicts of interest.

Consent to participate All authors have made a direct and intellectual contribution.

Consent for publication All authors approved the manuscript for publication.

References

Adonizio AL, Downum K, Bennett BC, Mathee K (2006) Anti-quorum sensing activity of medicinal plants in southern Florida. J Ethnopharmacol 105:427–435. https://doi.org/10.1016/j.jep.2005.11.025

Almeida FA, Pinto UM, Vanetti MCD (2016) Novel insights from molecular docking of SdiA from *Salmonella* Enteritidis and *Escherichia coli* with quorum sensing and quorum quenching molecules. Microb Pathog 99:178–190. https://doi.org/10.1016/j.micpath.2016.08.024

Almeida FA, Vargas ELG, Carneiro DG et al (2018) Virtual screening of plant compounds and nonsteroidal anti-inflammatory drugs for inhibition of quorum sensing and biofilm formation in *Salmonella*. Microb Pathog 121:369–388. https://doi.org/10.1016/j.micpath.2018.05.014

Askoura M, Saleh M, Abbas H (2020) An innovative role for tenoxicam as a quorum sensing inhibitor in *Pseudomonas aeruginosa*. Arch Microbiol 202:555–565. https://doi.org/10.1007/s00203-019-01771-4

Blosser RS, Gray KM (2000) Extraction of violacein from *Chromobacterium violaceum* provides a new quantitative bioassay for *N*-acyl homoserine lactone autoinducers. J Microbiol Methods 40:47–55. https://doi.org/10.1016/S0167-7012(99)00136-0

Boursier ME, Manson DE, Combs JB, Blackwell HE (2018) A comparative study of non-native *N*-acyl L-homoserine lactone analogs in two *Pseudomonas aeruginosa* quorum sensing receptors that share a common native ligand yet inversely regulate virulence. Bioorg Med Chem 26:5336–5342. https://doi.org/10.1016/j.bmc.2018.05.018

Burt SA, Ojo-Fakunle V, Woertman J, Veldhuizen EJA (2014) The natural antimicrobial carvacrol inhibits quorum sensing in *Chromobacterium violaceum* and reduces bacterial biofilm formation at sub-lethal concentrations. PLoS ONE 9:1–6. https://doi.org/10.1371/journal.pone.0093414

Capilato JN, Philippi S, Reardon T et al (2016) Development of a novel series of non-natural triaryl agonists and antagoinsts of the *Pseudomonas aeruginosa* LasR quorum sensing receptor. Bioorg Med Chem 25:153–165. https://doi.org/10.1016/j.bmc.2016.10.021

Chaudhari V, Gosai H, Raval S, Kothari V (2014) Effect of certain natural products and organic solvents on quorum sensing in *Chromobacterium violaceum*. Asian Pac J Trop Med 7:S204–S211. https://doi.org/10.1016/S1995-7645(14)60233-9

Chbib C (2020) Impact of the structure-activity relationship of AHL analogues on quorum sensing in Gram-negative bacteria. Bioorg Med Chem 28:115282. https://doi.org/10.1016/j.bmc.2019.115282

Chen G, Swem LR, Swem DL et al (2011) A strategy for antagonizing quorum sensing. Mol Cell 42:199–209. https://doi.org/10.1016/j.molcel.2011.04.003

Choi S-C, Zhang C, Moon S, Oh Y-S (2014) Inhibitory effects of 4-hydroxy-2,5-dimethyl-3(2H)-furanone (HDMF) on acyl-homoserine lactone-mediated virulence factor production and biofilm formation in *Pseudomonas aeruginosa* PAO1. J Microbiol 52:734–742. https://doi.org/10.1007/s12275-014-4060-x

Choi SH, Greenberg EP (1991) The C-terminal region of the *Vibrio fischeri* LuxR protein contains an inducer-independent *lux* gene activating domain. Proc Natl Acad Sci 88:11115–11119. https://doi.org/10.1073/pnas.88.24.11115

Choi SY, Yoon K, Il LJ, Mitchell RJ (2015) Violacein: properties and production of a versatile bacterial pigment. Biomed Res Int 2015:1–8. https://doi.org/10.1155/2015/465056

Choo JH, Rukayadi Y, Hwang J-K (2006) Inhibition of bacterial quorum sensing by vanilla extract. Lett Appl Microbiol 42:637–641. https://doi.org/10.1111/j.1472-765X.2006.01928.x

Dai L, Wu T, Xiong Y et al (2019) Ibuprofen-mediated potential inhibition of biofilm development and quorum sensing in *Pseudomonas aeruginosa*. Life Sci 237:116947. https://doi.org/10.1016/j.lfs.2019.116947

Das T, Sehar S, Koop L, Wong YK, Ahmed S, Siddiqui KS, Manefield M (2014) Influence of calcium in extracellular DNA mediated bacterial aggregation and biofilm formation. PLoS ONE 9(3):e91935. https://doi.org/10.1371/journal.pone.0091935

Ding T, Li T, Li J (2018) Identification of natural product compounds as quorum sensing inhibitors in *Pseudomonas fluorescens* P07 through virtual screening. Bioorg Med Chem 26:4088–4099. https://doi.org/10.1016/j.bmc.2018.06.039

El-Mowafy SA, Abd El Galil KH, El-Messery SM, Shaaban MI (2014) Aspirin is an efficient inhibitor of quorum sensing, virulence and toxins in *Pseudomonas aeruginosa*. Microb Pathog 74:25–32. https://doi.org/10.1016/j.micpath.2014.07.008

Ferreira DF (2011) Sisvar: a computer statistical analysis system. Cienc Agrotec 35:1039–1042. https://doi.org/10.1590/S1413-70542011000600001

Fuqua WC, Winans SC, Greenberg EP (1994) Quorum sensing in bacteria: the LuxR-LuxI family of cell density-responsive transcriptional regulators. J Bacteriol 176:269–275. https://doi.org/10.1128/JB.176.2.269-275.1994

Geske GD, O'Neill JC, Miller DM et al (2007) Modulation of bacterial quorum sensing with synthetic ligands: systematic evaluation of *N*-acylated homoserine lactones in multiple species and new insights into their mechanisms of action. J Am Chem Soc 129:13613–13625. https://doi.org/10.1021/ja074135h

Givskov M, de Nys R, Manefield M et al (1996) Eukaryotic interference with homoserine lactone-mediated prokaryotic signalling. J Bacteriol 178:6618–6622. https://doi.org/10.1128/JB.178.22.6618-6622.1996

Hanzelka BL, Greenberg EP (1995) Evidence that the N-terminal region of the *Vibrio fischeri* LuxR protein constitutes an autoinducer-binding domain. J Bacteriol 177:815–817. https://doi.org/10.1128/JB.177.3.815-817.1995

Harrison AM, Soby SD (2020) Reclassification of *Chromobacterium violaceum* ATCC 31532 and its quorum biosensor mutant CV026 to *Chromobacterium subtsugae*. AMB Express 10(1):202. https://doi.org/10.1186/s13568-020-01140-1

Howe TR, Iglewski BH (1984) Isolation and characterization of alkaline protease-deficient mutants of *Pseudomonas aeruginosa* in vitro and in a mouse eye model. Infect Immun 43(3):1058–1063. https://doi.org/10.1128/iai.43.3.1058-1063.1984

Inoue T, Shingaki R, Fukui K (2008) Inhibition of swarming motility of *Pseudomonas aeruginosa* by branched-chain fatty acids. FEMS Microbiol Lett 281:81–86. https://doi.org/10.1111/j.1574-6968.2008.01089.x

Li Z, Nair SK (2012) Quorum sensing: how bacteria can coordinate activity and synchronize their response to external signals? Protein Sci 21:1403–1417. https://doi.org/10.1002/pro.2132

Liu Z, Wang W, Zhu Y et al (2013) Antibiotics at subinhibitory concentrations improve the quorum sensing behavior of *Chromobacterium violaceum*. FEMS Microbiol Lett 341:37–44. https://doi.org/10.1111/1574-6968.12086

Mahmoudi E (2015) Signaling molecules from *Lactuca sativa* L. induced quorum sensing phenotypes in bacteria. J Plant Prot Res 55:166–171. https://doi.org/10.1515/jppr-2015-0022

Marathe K, Bundale S, Nashikkar N, Upadhyay A (2018) Influence of linoleic acid on quorum sensing in *Proteus mirabilis* and *Serratia marcescens*. Biosci Biotechnol Res Asia 15:661–670. https://doi.org/10.13005/bbra/2674

McClean KH, Winson MK, Fish L et al (1997) Quorum sensing and *Chromobacterium violaceum*: exploitation of violacein production and inhibition for the detection of *N*-acylhomoserine lactones. Microbiology 143:3703–3711. https://doi.org/10.1099/00221287-143-12-3703

Mion S, Carriot N, Lopez J, Plener L, Ortalo-Magné A, Chabrière E, Culioli G, Daudé D (2021) Disrupting quorum sensing alters social interactions in *Chromobacterium violaceum*. NPJ Biofilms Microbiomes 7(1):40. https://doi.org/10.1038/s41522-021-00211-w

Morohoshi T, Kato M, Fukamachi K et al (2008) *N*-Acylhomoserine lactone regulates violacein production in *Chromobacterium violaceum* type strain ATCC 12472. FEMS Microbiol Lett 279:124–130. https://doi.org/10.1111/j.1574-6968.2007.01016.x

Nealson KH, Platt T, Hastings JW (1970) Cellular control of the synthesis and activity of the bacterial luminescent system. J Bacteriol 104:313–322. https://doi.org/10.1128/JB.104.1.313-322.1970

Ng WL, Bassler BL (2009) Bacterial quórum sensing network architectures. Annu Rev Genet 43:197–222. https://doi.org/10.1146/annurev-genet-102108-134304

Nguyen Y, Nguyen NX, Rogers JL et al (2015) Structural and mechanistic roles of novel chemical ligands on the SdiA quorum-sensing transcription regulator. Mbio 6:1–10. https://doi.org/10.1128/mBio.02429-14

Oca-Mejía MM, Castillo-Juarez I, Martínez-Vázquez M, Soto-Hernandez M, Garcia-Contreras R (2015) Influence of quorum sensing in multiple phenotypes of the bacterial pathogen *Chromobacterium violaceum*. Pathog Dis 73(2):1. https://doi.org/10.1093/femspd/ftu019

Oliveira BDÁ, Rodrigues AC, Cardoso BMI et al (2016) Antioxidant, antimicrobial and anti-quorum sensing activities of *Rubus rosaefolius* phenolic extract. Ind Crops Prod 84:59–66. https://doi.org/10.1016/j.indcrop.2016.01.037

Parsek MR, Greenberg EP (2005) Sociomicrobiology: the connections between quorum sensing and biofilms. Trends Microbiol 13(1):27–33. https://doi.org/10.1016/j.tim.2004.11.007

Pejin B, Ciric A, Glamoclija J et al (2014) In vitro anti-quorum sensing activity of phytol. Nat Prod Res 29:374–377. https://doi.org/10.1080/14786419.2014.945088

Pérez-López M, García-Contreras R, Soto-Hernández M et al (2018) Antiquorum sensing activity of seed oils from oleaginous plants and protective effect during challenge with *Chromobacterium violaceum*. J Med Food 21:356–363. https://doi.org/10.1089/jmf.2017.0080

Pimentel-Filho NDJ, Martins MCDF, Nogueira GB, Mantovani HC, Vanetti MCD (2014) Bovicin HC5 and nisin reduce *Staphylococcus aureus* adhesion to polystyrene and change the hydrophobicity profile and Gibbs free energy of adhesion. Int J Food Microbiol 190:1–8. https://doi.org/10.1016/j.ijfoodmicro.2014.08.004

Pinto UM, Winans SC (2009) Dimerization of the quorum sensing transcription factor TraR enhances resistance to cytoplasmic proteolysis. Mol Microiol 73:32–42. https://doi.org/10.1111/j.1365-2958.2009.06730.x

Ponnusamy K, Paul D, Kim YS, Kweon JH (2010) 2(5H)-furanone: a prospective strategy for biofouling-control in membrane biofilm bacteria by quorum sensing inhibition. Brazilian J Microbiol 41:227–234. https://doi.org/10.1590/S1517-83822010000100032

Priyanka S, Priya JV, Rajesh SV et al (2015) Quorum sensing activity of *Couroupita guianesis* against *Enterobacter aerogens*: *in silico* studies. Int J Adv Sci Eng 1:1–6

Raina S, De VD, Odell M et al (2009) Microbial quorum sensing: a tool or a target for antimicrobial therapy? Biotechnol Appl Biochem 54:65–84. https://doi.org/10.1042/BA20090072

Ravichandran V, Zhong L, Wang H et al (2018) Virtual screening and biomolecular interactions of CviR-based quorum sensing inhibitors against *Chromobacterium violaceum*. Front Cell Infect Microbiol 8:1–13. https://doi.org/10.3389/fcimb.2018.00292

Reading C, Sperandio V (2006) Quorum sensing: the many languages of bacteria. FEMS Microbiol Lett 254:1–11. https://doi.org/10.1111/j.1574-6968.2005.00001.x

Shetye GS, Singh N, Gao X et al (2013) Structures and biofilm inhibition activities of brominated furanones for *Escherichia coli* and *Pseudomonas aeruginosa*. MedChemComm 4:1079–1084. https://doi.org/10.1039/c3md00059a

Singh VK, Mishra A, Jha B (2017) Anti-quorum sensing and antibiofilm activity of *Delftia tsuruhatensis* extract by attenuating the quorum sensing-controlled virulence factor production in *Pseudomonas aeruginosa*. Front Cell Infect Microbiol 7:1–16. https://doi.org/10.3389/fcimb.2017.00337

Soheili V, Bazzaz BSF, Abdollahpour N, Hadizadeh F (2015) Investigation of *Pseudomonas aeruginosa* quorum-sensing signaling system for identifying multiple inhibitors using molecular docking and structural analysis methodology. Microb Pathog 89:73–78. https://doi.org/10.1016/j.micpath.2015.08.017

Soni KA, Jesudhasan P, Cepeda M et al (2008) Identification of ground beef-derived fatty acid inhibitors of autoinducer-2-based cell signaling. J Food Prot 71:134–138. https://doi.org/10.4315/0362-028X-71.1.134

Srinivasan R, Devi KR, Kannappan A et al (2016) *Piper betle* and its bioactive metabolite phytol mitigates quorum sensing mediated virulence factors and biofilm of nosocomial pathogen *Serratia*

marcescens in vitro. J Ethnopharmacol 193:592–603. https://doi.org/10.1016/j.jep.2016.10.017

Srinivasan R, Santhakumari S, Ravi AV (2017) In vitro antibiofilm efficacy of *Piper betle* against quorum sensing mediated biofilm formation of luminescent *Vibrio harveyi*. Microb Pathog 110:232–239. https://doi.org/10.1016/j.micpath.2017.07.001

Stauff DL, Bassler BL (2011) Quorum sensing in *Chromobacterium violaceum*: DNA recognition and gene regulation by the CviR receptor. J Bacteriol 193:3871–3878. https://doi.org/10.1128/JB.05125-11

Vattem DA, Mihalik K, Crixell SH, McLean RJC (2007) Dietary phytochemicals as quorum sensing inhibitors. Fitoterapia 78:302–310. https://doi.org/10.1016/j.fitote.2007.03.009

Waters CM, Bassler BL (2005) Quorum sensing: cell-to-cell communication in bacteria. Annu Rev Cell Dev Bi 21:319–346. https://doi.org/10.1146/annurev.cellbio.21.012704.131001